Plant Syst Evol (2012) 298:1239–1247
DOI 10.1007/s00606-012-0630-8

ORIGINAL ARTICLE

Sites of self-pollen tube inhibition in Papaveraceae (sensu lato)

Paul Bilinski · Joshua Kohn

Received: 24 January 2012 / Accepted: 29 March 2012 / Published online: 19 April 2012

Abstract *Papaver rhoeas* (Papaveraceae) has a well-characterized gametophytic self-incompatibility system in which self-pollen tube growth ceases either just before, or just after, emergence from the copal aperture. *Papaver* flowers are unusual, however, in having flat stigmatic rays sitting directly on top of the hard ovary and no style. Immediate self-pollen arrest might be required with this floral architecture. There is much variation in floral architecture among Papaveraceae and self-incompatibility is widespread. However, there are no reports of the site of self-pollen tube inhibition in Papaveraceae other than *P. rhoeas*. We examined the site of self-pollen tube inhibition in four species (*Argemone munita*, *Lamprocapnos spectabilis*, *Eschscholzia californica*, and *Platystemon californicus*) representing a broad phylogenetic and morphological sample of Papaveraceae. Squash preparation was used for species with soft stigmas whereas woody tissue was sectioned with a cryostat and images were stitched into a mosaic to visualize pollen tubes on whole stigmas. For three species, self-pollen tube inhibition appeared similar to that described for *P. rhoeas*. Self-pollen tubes were arrested before any substantial penetration of female tissue and usually did not grow longer than 100 μm. In the fourth species, *A. munita*, self-pollen tubes grew up to 500 μm in length. However, self-pollen tubes appeared to grow along the stigmatic spines, and growth ceased once tubes contacted the stigma surface. Despite variation in floral architecture, rapid arrest of self-pollen tubes occurred before or just after penetration of female tissue in all species, consistent with the hypothesis that members of the family share the same incompatibility mechanism.

Keywords Self-incompatibility · Pollen tube inhibition · Papaveraceae · *Eschscholzia californica* · *Platystemon californicus* · *Argemone munita* · *Lamprocapnos spectabilis* · *Dicentra spectabilis*

P. Bilinski · J. Kohn (✉)
Department of Ecology, Behavior, and Evolution,
University of California, 9500 Gilman Drive, La Jolla,
San Diego, CA 92093-0116, USA
e-mail: jkohn@ucsd.edu

Present Address:
P. Bilinski
Department of Plant Sciences, University of California Davis,
One Shields Avenue, Davis, CA 95616, USA

Introduction

Self-incompatibility, the ability of many plants to recognize and reject their own pollen to avoid the deleterious effects of self-fertilization, is found in many plant families (Weller et al. 1995; Igic et al. 2008). Many different forms of self-incompatibility are known and, in a few cases, the molecular mechanisms involved have been at least partially elucidated (Franklin-Tong 2008). Nevertheless, information on the sites of self-pollen tube inhibition or the genetics of incompatibility remains incomplete for many plant groups.

In single locus gametophytic self-incompatibility (GSI), haploid pollen is rejected if the allele it carries at the self-incompatibility (*S*-) locus matches either allele present in the diploid female reproductive tissue (de Nettancourt 1977). Two systems of GSI have been characterized at the molecular level. In the Rosaceae, Plantaginaceae, and Solanaceae, the stylar product of the *S*-locus responsible for self-pollen rejection is an RNase (*S*-RNase; McClure et al. 1990) whereas the pollen-expressed proteins it interacts with are believed to be F-box proteins known as

SLF or SFB (Entani et al. 2003; Ushijima et al. 2004; Ikeda et al. 2004; Qiao et al. 2004; Sijacic et al. 2004; Sassa et al. 2007; Kubo et al. 2010). In *S*-RNase based self-incompatibility, self-pollen grains germinate and their tubes extend into the stigma, but growth is typically retarded in the distal third of the style. A different molecular mechanism of GSI, known as the *S*-glycoprotein model, is documented for *Papaver rhoeas* (Papaveraceae; Foote et al. 1994; Franklin-Tong 2008; Wheeler et al. 2009). Both pistil and pollen *S*-locus recognition proteins in *P. rhoeas* have been isolated and these bear no homology to the *S*-RNase/SLF-SFB system. The female component of the system is a small ($\sim$15 kDa) secreted peptide that binds to a recently characterized pollen-expressed receptor (Wheeler et al. 2009). In *P. rhoeas*, self-pollen tubes cease growth very soon after hydration. Some self-pollen tubes never emerge from the colpal aperture and most are arrested immediately on contact with the stigma (Franklin-Tong and Franklin 1993; Franklin-Tong 2008).

Self-pollen tube inhibition in *P. rhoeas* is believed to result from initiation of a signaling cascade that leads to rapid programmed cell death (PCD; Thomas and Franklin-Tong 2004). It is clear that in *P. rhoeas* self-pollen recognition occurs directly on the surface of the stigma before penetration of the pollen tube into the female tissue. Once pollen is identified as self, the cascade of inhibition begins with a change in the Ca^{2+} gradient within the shaft of the pollen tube (Franklin-Tong et al. 1993). This is followed by reactions that lead to breakdown of the F-actin cytoskeleton of the pollen tube. Flux of the calcium gradient is known to trigger the phosphorylation that inhibits the function p26, a Mg^{2+}-dependent sPPase (Rudd et al. 1996). This enzyme has a vital function in pollen tube elongation. When p26 is phosphorylated and its activity is reduced, the cascade results in inhibition of many biosynthetic pathways including those involved in pollen tube elongation (de Graaf et al. 2006). Early triggering of this cascade may explain why only very short pollen tubes are observed. When inhibition of p26 stops the pollen tube from elongating, the change of the Ca^{2+} gradient begins the pathway, leading to PCD (Thomas and Franklin-Tong 2004). The process of PCD is accomplished via fragmentation of the DNA of the incompatible pollen. This effect of the change of the calcium gradient completes the process of incompatible pollen inhibition at the stigma surface.

Papaver rhoeas has an unusual floral structure with stigma rays sitting directly on top of the rather hard ovary (Fig. 1). The immediate stigmatic inhibition of pollen tube growth observed in *P. rhoeas* may result from the species' lack of a style or alternative tissues for self-pollen arrest. Among Papaveraceae (sensu lato, including Fumariaceae), many of which are self-incompatible (Beatty 1936; Cook 1962; Hannan 1981; Paape et al. 2011), there is much

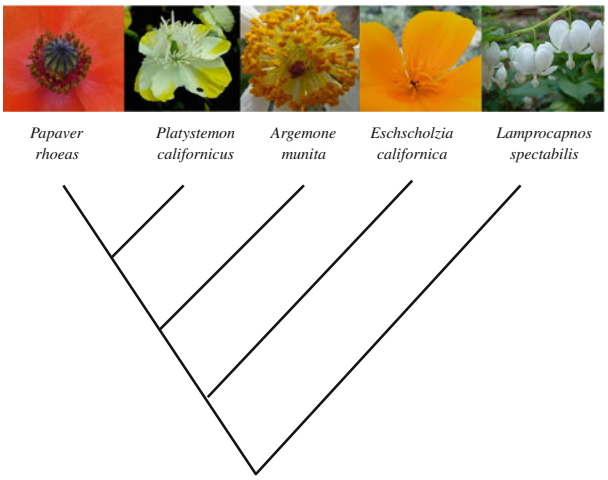

Fig. 1 Floral diversity of Papaveraceae (sensu lato) examined in this study. Phylogenetic relationships are redrawn from Hoot et al. (1997)

variation in the structure of female floral tissues (Fig. 1). However, there are no reports of the site of inhibition of self-pollen outside *Papaver*. For instance, self-incompatible *Platystemon californicus* (Hannan 1981; Paape et al. 2011) has several long soft stigmas that extend upward from the ovary (Fig. 1). Another self-incompatible species, *Argemone munita* (Paape et al. 2011) has woody stigmas fused into a central mass. Flowers of the self-incompatible California poppy, *Eschscholzia californica* (Beatty 1936; Cook 1962), have four thin, soft, linear stigmas extending out of the ovary. *Lamprocapnos* (formerly *Dicentra*) *spectabilis* has a style subtending its arrowhead-shaped stigma. These species encompass a wide phylogenetic sample of Papaveraceae (Hoot et al. 1997) and have a variety of floral morphologies and potential sites for self-pollen inhibition. Here we examine the site of self-pollen tube inhibition by use of microscopy.

Materials and methods

Plant material

Seeds of *P. californicus* were collected from: Lake Cuyamaca State Park east of San Diego (N 32°58′ 59.1″, W 116° 33′ 45.4″), Hastings Natural History Reserve (N 36° 23′07.1″, W 121° 33′ 16.6″), and along the side of Carmel Valley Road near Carmel, CA, USA (N 36° 26′34.5″, W 121° 38′ 53.7″). Individuals of *A. munita* were originally collected as seeds from Valentine Eastern Sierra Reserve (N 37°56′ 52.1″ W 118°49′ 31.7″), Mammoth Lakes, CA, USA, and Emerson Oaks UC Reserve (N 33°28′ 22.9″ W 117°19′ 34.9″) near Temecula, CA, USA. These seeds were used for greenhouse crosses. All seeds for *A. munita* and *P. californicus* were placed in 1″ plug trays in moist Sungro

professional mix for germination. Seeds in trays were exposed to cold treatment at 4 °C for 45–90 days. Germination success was very low. Seedlings of *A. munita* were grown in natural light conditions in a glasshouse whereas *P. californicus* seedlings were grown under fluorescent lights in 14/10 h day/night cycles.

Seeds of *E. californica* were collected from Antelope Valley, Los Angeles, CA, USA (N 34°43′ 29 W 118°23′ 54.6″) and from commercial seed sources. Seeds were placed in a sealed Petri dish on top of moist filter paper and kept in the dark for 72 h. All seeds showing a radical (>90 %) were then transferred into wet soil in small pots. Seedlings were grown under fluorescent light in 14/10 h day/night cycles in a growth chamber. Juvenile plants were then transferred to potting soil and moved to the glasshouse and natural light conditions to support flowering. Individuals of *L. spectabilis* var. *alba* were purchased as potted plants from a local nursery. All species used in this study were known to be self-incompatible (Beatty 1936; Cook 1962; Hannan 1981; Paape et al. 2011) except *L. spectabilis* whose incompatibility status was confirmed by hand self and cross-pollination.

Pollinations

Flowers were bagged before opening and emasculated before anthesis. Anthers containing pollen were then taken from another open flower on the same plant for self-pollinations, or from another plant for cross-pollinations, and brushed against the stigma of the flower until pollen was visible. Bags over the flowers were then replaced.

Slide preparation

For species having soft stigma tissue (*P. californicus*, *L. spectabilis*, *E. californica*), squash preparations were used, whereas the woody stigmas of *A. munita* were prepared with both squash preparations and cryostat sectioning. For squash preparations, stigma tissue was removed from the plant 24 h after pollination and placed in a −75 °C freezer for storage or prepared immediately for microscopy. For microscopy, stored tissue was thawed at room temperature for 30 min and submerged in 500 μM aniline blue stain (0.2 g aniline blue, 20 g tripotassium orthophosphate, 1 L distilled water). Aniline blue fluoresces on binding to β-1,3-glucan, more commonly known as callose, an essential polysaccharide in the cell walls of pollen tubes. Stigmas were then placed on slides, surrounded in petroleum jelly to prevent loss of stain, squashed using the cover-slip, and sealed with clear nail polish.

For cryostat sectioning, whole gynoecia were trimmed from flowers 24 h after pollination. Sagittal or transverse sections were cut through the stigma tissue by use of a razor blade. Stigma halves were placed in a tray and submerged in Tissue-Tek® O.C.T.™ (Sakura) for 10–20 min to enable penetration. Samples were then frozen in 2-methylbutane pre-cooled in liquid nitrogen and placed in a cryostat with a chamber temperature of −14 °C. After being left to warm to this temperature, 100 μm sections were cut. Samples were placed on poly-L-lysine-coated slides, encased in liquid plastic embedding resin, and left to dry in air for approximately 24 h. Slides were then rehydrated in 50 μL aniline blue solution for 20 min. The solution was removed and samples were then washed in phosphate-buffered saline (0.145 M NaCl, 0.01 M phosphate, pH 7.1) twice to remove any unbound fluorophores. Final treatment with Gelvatol (1:2 polyvinyl alcohol:glycerol) was used to preserve fluorescence before the sample was sealed with a cover-slip and clear nail polish.

Imaging

Images from squash preparations were captured using an excitation filter of 510–560 nm and a Nikon Eclipse E600 fluorescent microscope with a 10× Nikon objective. This enabled callose fluorescence (509 nm) and some autofluorescence (approximately 520 nm) to pass. Stitched mosaic images from cryostat sections were gathered using an Olympus DSU confocal microscope with dapi and alexafluor filters (transmittance 365 and 488 nm, respectively), a Hamamatsu EMCCD camera, and an automated XYZ stage. Panels were stitched together by use of Neurolucida® software.

Results

Numbers of stigmas examined after self and cross pollinations are given in Table 1. In all cases, observed pollen tube behavior was quite consistent among crosses of the same type and species. For three species, *E. californica*, *L. spectabilis*, and *P. californicus* (Figs. 2, 3, 4) the phenotype was consistent with pollen behavior previously documented for *P. rhoeas*. For *E. californica*, self-pollen grains did not extend tubes into the soft long linear stigma whether deposited near the proximal (Fig. 2a) or distal (Fig. 2c) regions. After cross-pollinations, pollen tubes were clearly present at the base of the stigma tissue. Cross-pollen tubes in *E. californica* were able to penetrate into the interior of the stigma after deposition anywhere along it.

Lamprocapnos spectabilis self-pollen grains extended short tubes in many directions at the surface of the stigma, but growth was never seen to extend more than a tenth of a millimeter into the stigma tissue in the direction of the style (Fig. 3a). In contrast, outcross-pollen grains deposited on

Table 1 Numbers of self and cross-pollinations observed for pollen tube growth and for seed set

Species	Number of stigmas observed under microscope		Number of pollinations observed for fruit set	
	Self	Cross	Self	Cross
P. californicus	17	14	22 (0)	60 (56)
E. californica	16	8	30 (0)	15 (15)
A. munita	8	6	61 (7)	64 (64)
L. spectabilis	5	5	6 (0)	5 (5)

Numbers in parentheses indicate the number of crosses producing fruit. Fruit-set data after self and cross-pollinations for *Argemone munita* and *Platystemon californicus* are from Paape et al. (2011). Occasional seed-set after self-pollination of *A. munita* was apparently because of a weak or non-functional incompatibility allele [further details are given by Paape et al. (2011)]. This allele was not involved in any of the crosses used for observing pollen tube growth

all sides of the stigmatic surface extended tubes toward a central position on the stigma tissue and through it into the style (Fig. 3b).

Platystemon californicus self-pollen extends short (usually <50 μm) tubes toward the interior of the stigma tissue but tubes fail to elongate further (Fig. 4). Inhibition occurs before substantial penetration of the stigma. Whereas germination after self and cross-pollination appears similar (Fig. 4a, b), outcross pollen tubes extend into and then towards the distal end of the linear stigma (Fig. 4d). Figure 4c, d show that after self-pollination, no tubes extend to the distal end of the stigma and pollen deposited at the distal end is also inhibited. In contrast, many pollen tubes are observed at the distal end of the stigma after cross-pollination.

For *Argemone munita* self-pollen tubes the phenotype is different from that of other species examined (Figs. 5, 6). Initial pollen tube growth appears similar after either self or cross-pollination (Fig. 5a, b) with self-pollen tubes extending several hundred microns, much further than seen for the other species. However, using the method of cryostat sectioning and mosaic stitching, differences after self and cross-pollination are visible. In mosaic stitched images, callose fluorescence appears blue whereas auto-fluorescence of other tissues is green. In Fig. 5c, no callose fluorescence from pollen tubes is present beyond a thin, well-defined, layer representing the surface of the stigma at the base of the spiny hairs that project upward from it, whereas tubes from cross-pollen (Fig. 5d) extend further into the interior. Deposition occurs on the stigma spines and self-pollen tubes apparently extend down along these

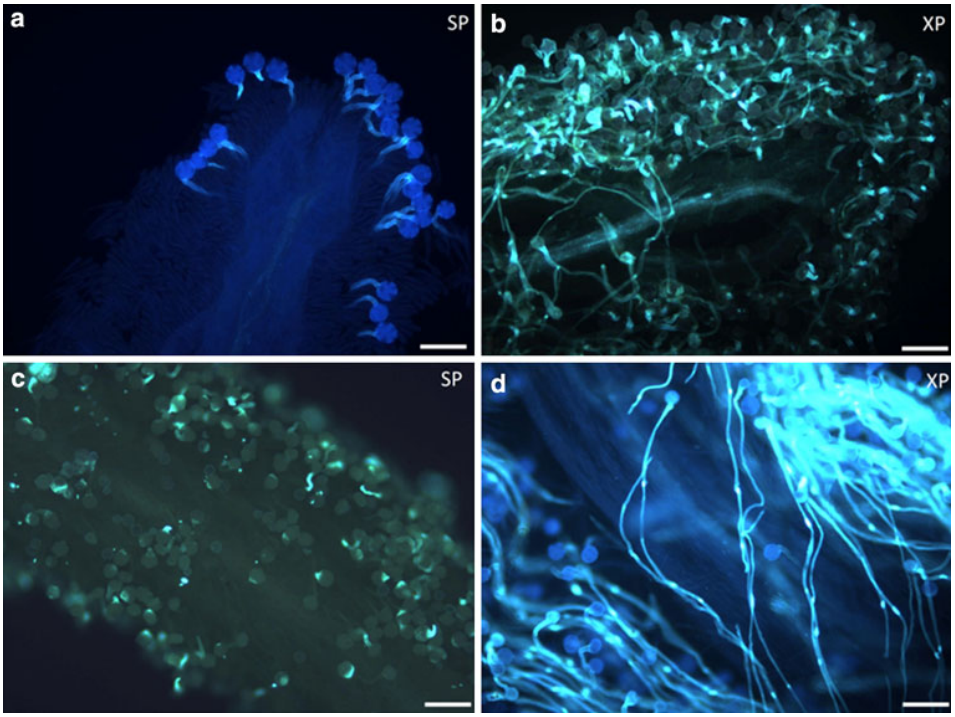

Fig. 2 Fluorescent light microscopy images of squash preparations of stigma tissue from *Eschscholzia californica* after exposure to self, *SP*, and outcross, *XP*, pollen. **a**, **b** Images of the proximal ends of stigma tissue exposed to different pollen treatment. Pollen tubes extend into the stigma tissue only after cross-pollination. **c**, **d** Images of the distal ends of stigma tissue exposed to different pollen treatment. Pollen tube penetration continues in the direction of the ovaries in the case of cross-pollination. *Scale bar* 100 μm

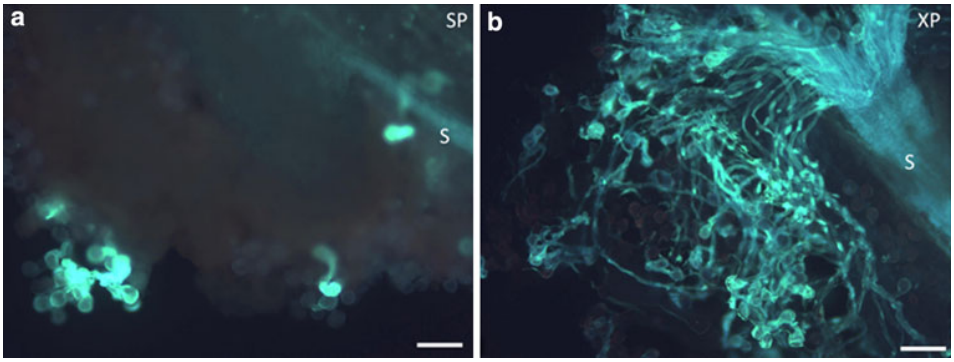

Fig. 3 Fluorescent light microscopy images of squash preparations of stigma tissue from *Lamprocapnos spectabilis* after deposition of self and outcross pollen. **a** Self-pollen, *SP*, tubes do not elongate into the tissue. **b** Cross-pollen, *XP*, tubes grow in large numbers toward the style *S*. *Scale bar* 100 μm

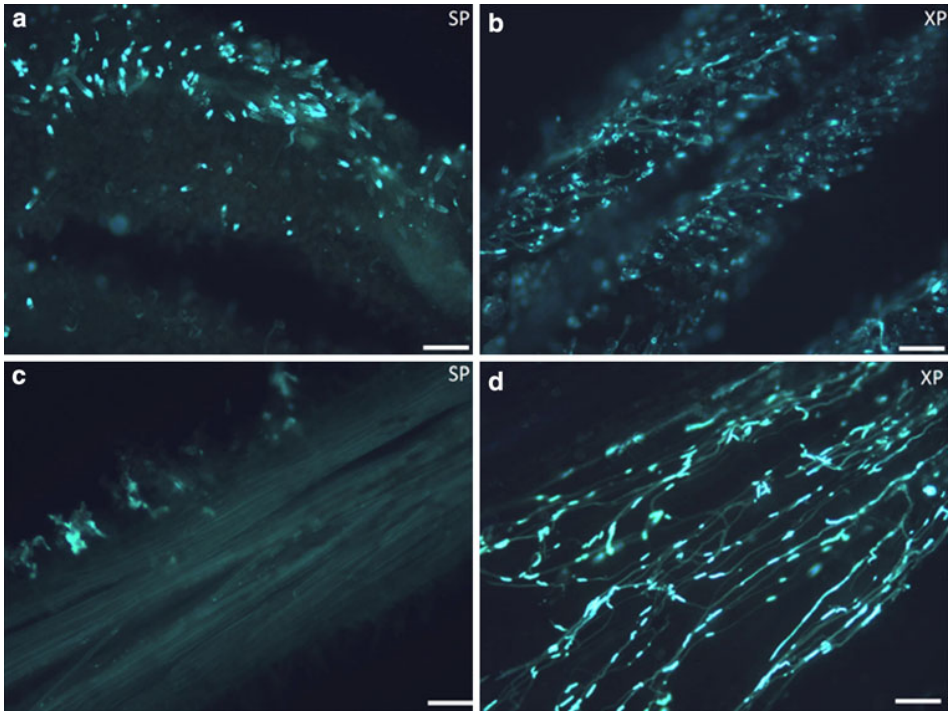

Fig. 4 Fluorescent light microscopy images of stigma tissue from *Platystemon californicus* after exposure to outcross pollen, *XP*, and self-pollen, *SP*. Tissue was fixed by use of squash preparation. **a**, **b** Images of the proximal end of stigmas. Pollen tube growth after both treatments appears fragmented, although fragments appear longer after cross-pollination. **c**, **d** Images of the distal end of stigmas. Pollen tubes are only present and elongating after cross-pollination treatment. *Scale bar* 100 μm

to the stigma surface where they are interrupted, whereas cross-pollen tubes continue to extend through this layer and on toward the ovary.

Further information can be extracted when examining full stitched mosaic images of stigmata (Fig. 6). These show that self-pollen tube inhibition occurs before entry into stigma tissue below the surface spines (Fig. 6a, c). The tubes from outcross pollen penetrate the stigma tissue and grow beyond this barrier (Fig. 6b). Cross-pollen tubes extend to the distal end of the stigma and down the transmission tract (Fig. 6b). The mass of pollen tubes in blue follow a common path toward the ovary, a phenotype that was not observed after self-pollination (Fig. 6a, c).

Discussion

Despite substantial differences in floral morphology among self-incompatible members of the Papaveraceae (sensu lato), self-pollen tube inhibition in all species examined occurred shortly after contact with female tissue, consistent with pollen tube behavior previously observed for *P. rhoeas* (Franklin-Tong 2008). In *L. spectabilis*, *E. californica*, and *P. californicus*, self-pollen tubes were arrested at the surface of the stigma and did not penetrate more than 100 μm. The only exception among the Papaveraceae examined occurred in *A. munita* which has a woody stigma covered with a dense mat of spines. Self-pollen tubes

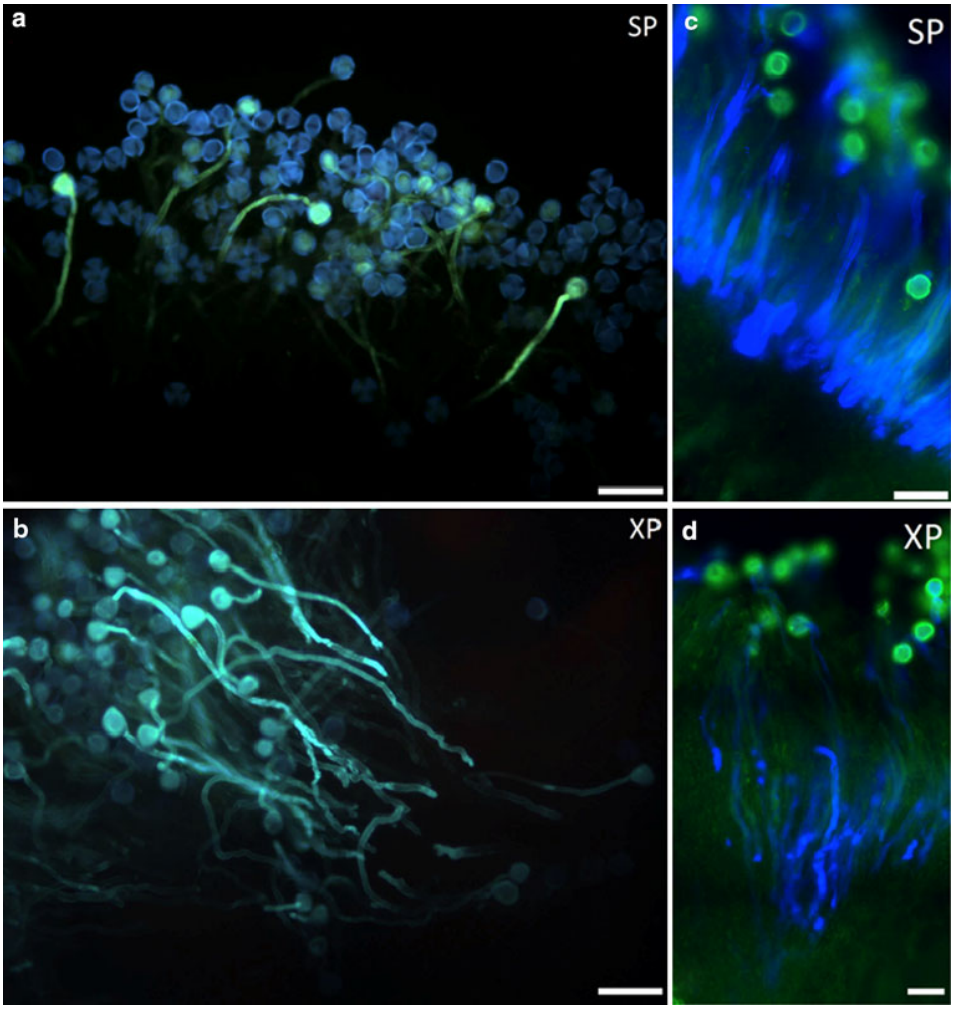

Fig. 5 Fluorescent light microscopy images of stigma tissue from *Argemone munita* after exposure to outcross pollen, *XP*, and self-pollen, *SP*. **a**, **b** were prepared with squash preparation. **c**, **d** are zoomed-in images of stitched mosaics prepared with cryostat sectioning. In stitched mosaics, wavelength coloration was added so that pollen tubes (emitting at 509 nm) appear *blue*. Another image was captured to show plant tissue auto-fluorescence which emitted at 520 nm. This was colored *green*. *Scale bar* 100 µm

extended through the spiny layer, apparently between the spines, before being arrested at an auto-fluorescent layer representing the stigma surface. Therefore, in no case were self-pollen tubes able to grow more than 100 µm within female tissue.

The variable flower morphologies among species examined formed two different groupings: species with thin, soft stigmas (*E. californica*, *P. californicus, L. spectabilis*) and species with spiny, woody female tissue (*A. munita*). Squash preparations were sufficient to observe the site of pollen tube inhibition for all species with soft female tissue (*E. californica*, *P. californicus* and *L. spectabilis*). Cryostat preparations and stitched mosaic imaging were needed to observe the site of self-pollen tube inhibition for *A. munita*.

The consistency observed in the site of inhibition of pollen tubes suggests the maintenance of the same SI mechanism across Papaveraceae (sensu lato). Self-incompatibility has arisen independently several times in angiosperms. For instance, some closely related families have different types of homomorphic self-incompatibility (e.g. gametophytic SI in Solanaceae and sporophytic SI in Convolvulaceae; Igic et al. 2008). However, in only one instance is there evidence of more than one form of homomorphic incompatibility within a plant family. Crossing experiments suggest that two different species of Polemoniaceae, *Linanthus parviflorus* and *Phlox drummondii*, maintain gametophytic and sporophytic self-incompatibility systems, respectively (Levin 1993; Goodwillie 1997). It should be noted that the sites of self-pollen tube arrest are similar for these two species, suggesting morphological evidence may not be definitive for assessing common molecular mechanisms. However, in the Papaveraceae, recent work (Paape et al. 2011) found crossing results for *A. munita* and *P. californicus* that were

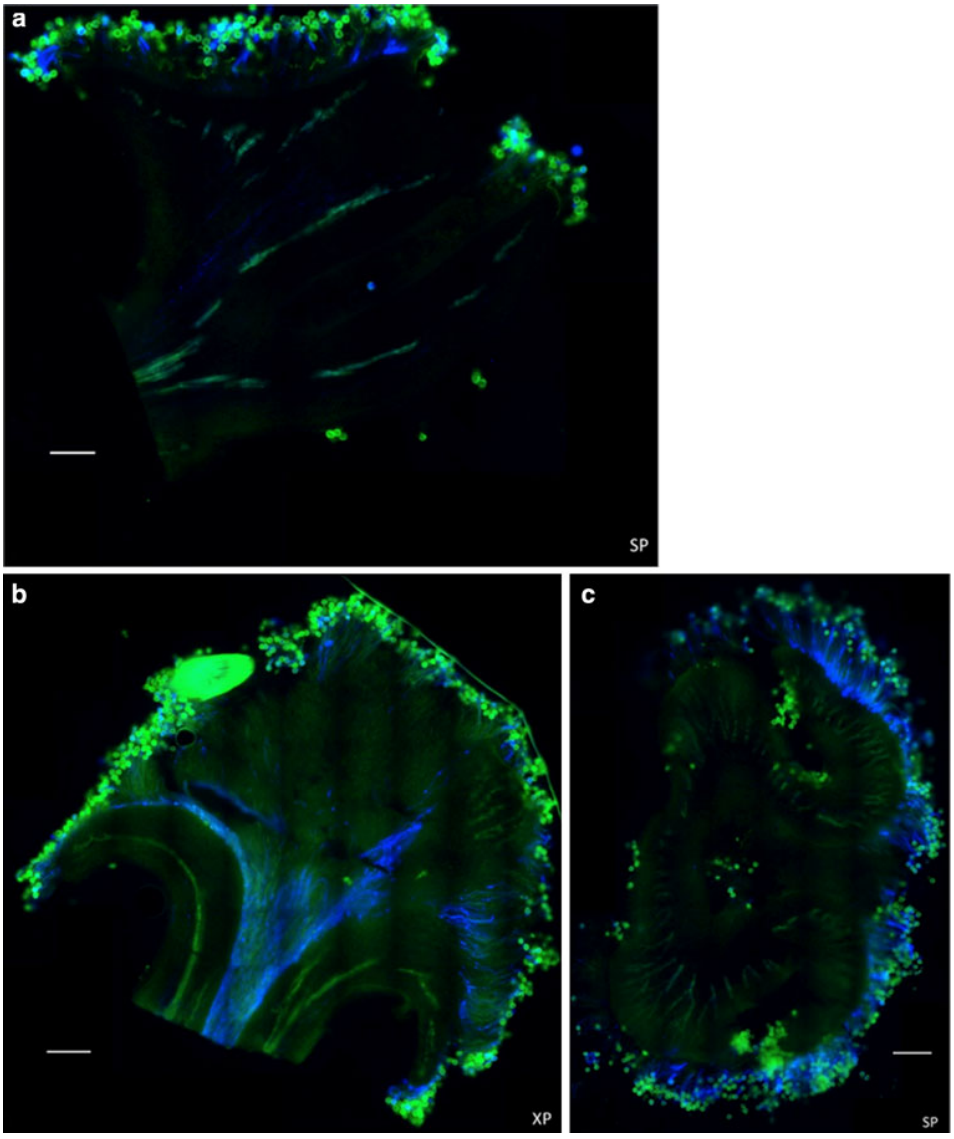

Fig. 6 Fluorescent light microscopy images of sectioned stigma tissue from *Argemone munita* after exposure to outcross pollen, *XP*, and self-pollen, *SP*. Images are stitched mosaics. **a**, **b** Sagittal sections of stigma tissue. Penetration of pollen tubes (*blue*) into the style occurs only after cross-pollination. **c** Transverse section of stigma tissue from individual 8–4 after self-pollination. Pollen tubes (*blue*) end before penetrating through the stigma. *Scale bar* 500 μm

consistent with a gametophytic basis of self-incompatibility. In addition, homologs of the *S*-alleles of *Papaver* were found that were expressed in female tissue. Putative *S*-locus genotype was correlated with incompatibility phenotype, suggesting these homologs might be functional *S*-alleles and that the molecular basis of self-incompatibility of these two species is homologous with *Papaver*. However using the same PCR methods, no *S*-locus sequence information was obtained from *E. californica* (T. Paape and J. R. Kohn, unpublished data), perhaps because it is more distantly related to *Papaver* (Hoot et al. 1997; Fig. 1) than are either *P. californicus* or *A. munita*. Such experiments have not been attempted with *L. spectabilis*, which is even more distantly related to *Papaver*. Obtaining sequence information from *E. californica* and *L. spectabilis,* perhaps by next-generation sequencing of the stigmatic transcriptome, would strengthen the inference of a single basis of GSI among Papaveraceae (sensu lato).

In addition to analysis of pollen tube growth and inhibition, this study tested the usefulness of methods other than squash preparation for pollen tube observation. Squash preparation causes tissues to shift. This was especially true for *A. munita*, for which squash preparation showed that self-pollen tubes were not inhibited early and that self-pollen tube length was much greater than recorded for other species (Fig. 5a, c). With squash preparations of

this species, self-pollen tube inhibition appeared to occur at random locations in the stigma rather than immediately after contact with or attempted penetration of living female tissue. When examining cross-pollinations, squash preparation showed tubes growing everywhere within female tissues, unlike observations for *P. rhoeas*, in which cross-pollen tubes funnel down a central transmission tract (Franklin-Tong and Franklin 1993).

In contrast, cryostat preparation maintained the pollen tubes in place, enabling better imaging, particularly of thicker and woodier tissues. Structures such as the transmitting tract and stigma surface, which were lost in squash preparation, were visible through cryostat sectioning. The large, thick nature of these tissues in *A. munita* necessitated the use of mosaics rather than single panel micrographs to accurately capture the pattern of pollen tube elongation. Because all cross-pollen tubes and some self-pollen tubes extended beyond a single field of view, stitched mosaics had the benefit of enabling pollen tube growth to be traced through the tissue by use of automated image-capture techniques. Cryostat sectioning, by preserving the orientation of tubes across the entire stigma, enabled us to see that self-pollen tubes have a common, well-defined, site of inhibition (Fig. 6). These techniques also enabled us to visualize cross-pollen tubes extending into the transmission tract of *A. munita*, another piece of information lost in squash preparation.

In conclusion, this study extends our knowledge of the sites of self-pollen tube inhibition among Papaveraceae (sensu lato). Images comparing self and outcross pollination in *A. munita*, *L. spectabilis*, *E. californica*, and *P. californicus* found that in all species except *A. munita* self-pollen tube arrest occurred immediately on contact with female tissue. In *A. munita*, contact with the long stigma spines did not arrest self-pollen tubes but their growth did halt immediately after tubes reached the stigma surface at the base of the spines. Cryostatic sectioning proved essential for visualizing the site of inhibition in *A. munita*, for which squash preparations failed to maintain tissue integrity and pollen tube orientation. This technique is likely to be useful for other taxa, particularly those with large masses of woody stigma tissue.

Acknowledgments This study was supported by National Science Foundation award DEB 0639984 to JRK. We thank the staff at the National Center for Microscopy and Imaging Research for help with microscopy and T. Paape for useful discussion and advice.

References

Beatty AV (1936) Genetic studies of the California poppy. J Hered 47:331–338

Cook SA (1962) Genetic system, variation, and adaptation in *Eschscholzia californica*. Evolution 16:278–299

de Graaf BHJ, Rudd JJ et al (2006) Self-incompatibility in *Papaver* targets soluble inorganic pyrophosphatases in pollen. Science 444:490–493

de Nettancourt D (1977) Incompatibility in angiosperms. Springer, New York

Entani T, Iwano M, Shiba H, Che FS, Isogai A, Takayama S (2003) Comparative analysis of the self-incompatibility (*S*-) locus region of *Prunus mume*: identification of a pollen-expressed F-box gene with allelic diversity. Genes Cells 8:203–213

Foote HG, Ride JP, Franklin-Tong VE, Walker EA, Lawrence MJ, Franklin FCH (1994) Cloning and expression of a distinctive class of self-incompatibility (S) gene from *Papaver rhoeas*. Proc Natl Acad Sci USA 91:2265–2269

Franklin-Tong VE (2008) Self-incompatibility in *Papaver rhoeas*: progress in understanding mechanisms involved in regulating self-incompatibility in *Papaver*. In: Franklin-Tong VE (ed) Self-incompatibility in flowering plants: evolution, diversity, and mechanisms. Springer, Heidelberg, pp 237–258

Franklin-Tong VE, Franklin FCH (1993) Gametophytic self-incompatibility: contrasting mechanisms for *Nicotiana* and *Papaver*. Trends Cell Biol 3:340–345

Franklin-Tong VE, Ride JP, Read ND, Trewawas AJ, Franklin FCH (1993) The self-incompatibility response in *Papaver rhoeas* is mediated by cytosolic free calcium. Plant J 4:163–177

Goodwillie C (1997) The genetic control of self-incompatibility in *Linanthus parviflorus* (Polemoniaceae). Heredity 79:424–432

Hannan GL (1981) Flower color polymorphism and pollination biology of *Platystemon californicus* Benth. (Papaveraceae). Am J Bot 68:233–243

Hoot SB, Kaderiet JW, Blattner FR, Jork KB, Schwarzbach AE, Crane PR (1997) Data congruence and phylogeny of the Papaveraceae s.l. based on four data sets: *atpB* and *rbcL* sequences, *trnK* restriction sites and morphological characters. Syst Bot 22:575–590

Igic B, Lande R, Kohn JR (2008) Loss of self-incompatibility and its evolutionary consequences. Int J Plant Sci 169:93–104

Ikeda K, Igic B, Ushijima K et al (2004) Primary structural features of the *S* haplotype-specific F-box protein, *SFB*, in *Prunus*. Sex Plant Reprod 16:235–243

Kubo K, Entani T, Takara A et al (2010) Collaborative non-self recognition system in S-RNase-based self-incompatibility. Science 330:796–799

Levin DA (1993) *S*-gene polymorphism in *Phlox drummondii*. Heredity 71:193–199

McClure BA, Gray JE, Anderson MA, Clarke AE (1990) Self-incompatibility in *Nicotiana alata* involves degradation of pollen rRNA. Nature 250:937–941

Paape T, Miyake T, Takebayashi N, Wolf D, Kohn JR (2011) Evolutionary genetics of an S-like polymorphism in Papaveraceae with putative function in self-incompatibility. PLoS ONE. doi:10.1371/journal.pone.0023635

Qiao H, Wang F, Zhao L et al (2004) The F-box protein *AhSLF-S2* controls the pollen function of S-RNase-based self-incompatibility. Plant Cell 16:2307–2322

Rudd JJ, Franklin CH, Lord JM, Franklin-Tong VE (1996) Increased phosphorylation of a 26-kD pollen protein is induced by the self-incompatibility response in *Papaver rhoeas*. Plant Cell 8:713–724

Sassa H, Kakui M, Miyamoto Y et al (2007) *S*-locus F-box brothers: multiple pollen-specific F-box genes with *S* haplotype-specific polymorphisms in apple and Japanese pear. Genetics 175: 1869–1881

Sijacic P, Wang X, Skirpan AL et al (2004) Identification of the pollen determinant of S-RNase mediated self-incompatibility. Nature 429:302–305

Thomas SG, Franklin-Tong VE (2004) Self-incompatibility triggers programmed cell death in *Papaver* pollen. Nature 429:305–308

Ushijima K, Yamane H, Watari A et al (2004) The *S* haplotype-specific F-box protein gene, *SFB*, is defective in self-compatible haplotypes of *Prunus avium* and *P. mume*. Plant J 39:573–586

Weller SG, Donoghue MJ, Charlesworth D (1995) The evolution of self-incompatibility in flowering plants: a phylogenetic approach. In: Hoch PC, Stephenson AG (eds) Experimental and molecular approaches to plant biosystematics. Missouri Botanical Garden, St. Louis, pp 355–382

Wheeler MJ, de Graaf BHJ, Hadjiosif N et al (2009) Identification of the pollen self-incompatibility determinant in *Papaver rhoeas*. Nature 459:992–995